

## Influence of Magnetic Agitation and Bubble Stirring on Electrodeposited Copper in an Acidic CuSO<sub>4</sub> Solution

Changlu Shan<sup>1,2</sup>, Qiushi Song<sup>1,2,\*</sup>, Hongwei Xie<sup>1,2,\*</sup>, Zhiqiang Ning<sup>1,2</sup>

<sup>1</sup> School of Metallurgy, Northeastern University, Shenyang 110819, China

<sup>2</sup> Liaoning Key Laboratory for Metallurgical Sensor and Technology, Northeastern University, Shenyang 110819, China

\*E-mail: [songqs@smm.neu.edu.cn](mailto:songqs@smm.neu.edu.cn), [xiehw@smm.neu.edu.cn](mailto:xiehw@smm.neu.edu.cn)

Received: 16 December 2020 / Accepted: 27 January 2021 / Published: 28 February 2021

Electrochemical reduction is an effective method to transform Cu<sup>2+</sup> ions into metallic Cu in aqueous solutions. Herein, magnetic agitation and flowing bubbles were introduced into the electrowinning process of Cu<sup>2+</sup> ions in a CuSO<sub>4</sub>-H<sub>2</sub>SO<sub>4</sub> electrolyte. The influence of agitation and micron-sized bubbles on the nucleation and growth of Cu electrodeposits was systematically investigated. Additionally, the composition and microstructure of the Cu deposits were analyzed. The migration of Cu<sup>2+</sup> ions towards the cathode was effectively accelerated by agitation and bubbles. Cu dendrites can be basically eliminated in the product. Primary nucleation and the subsequent growth of the Cu electrodeposits were effectively promoted, while secondary nucleation of Cu was suppressed. Finally, compact and homogeneous Cu electrodeposits were prepared by employing agitation and flowing bubbles to assist the electrowinning of Cu ions.

**Keywords:** Electrowinning; copper; magnetic agitation; flowing bubble; kinetics

### 1. INTRODUCTION

Metallic copper (Cu) presents many excellent properties, including good thermal and electrical conductivity, chemical stability and excellent creep resistance. Therefore, it is widely used in various fields such as construction and infrastructure materials, circuit boards and wires in the information, electronic component and electronic industries [1-5]. The properties of Cu (resistivity, mechanical properties, etc.) highly depend on the levels of purities inside (bismuth, antimony, arsenic and stannum, etc.) [2, 3, 6-8]. Thus, high-purity (more than 99.999 wt. %) Cu is often desired in some special applications, such as sputtering targets and electronic components.

Electrochemical reduction is an essential procedure to transform Cu<sup>2+</sup> ions into metallic Cu in

the pyrometallurgical or hydrometallurgical treatment of copper ores. Electrolytic Cu (more than 99 wt. %) can be produced by electrowinning  $\text{Cu}^{2+}$  ions or electrorefining blister copper in aqueous solutions [2]. In addition, the electrowinning process is also utilized to produce high-purity Cu [9]. However, some challenges still exist to produce high-quality Cu electrodeposits. For example, Cu deposits produced from electrowinning or electrorefining processes often have a nodular and porous morphology [10]. This morphology induces the aggregation of impurities at the boundaries and the formation of voids in the deposits. Therefore, the concentration and distribution of impurities are closely related to the characteristics of Cu electrodeposits (morphology, microstructure, crystal orientation, etc.). Organic additives such as gelatin and thiourea are often added into the electrolyte to produce smooth deposits with finer grains [11-14]. Moreover, the inclusion of impurities from floating slime can be suppressed during the electrowinning process. However, the introduction of these additives has a negative effect on the purity of Cu deposit, which is especially obvious in the preparation of high-purity Cu. The quality of the Cu product is associated with the circumstance around the cathode, such as diffusion of Cu ions, thickness of diffusion layer and absorption of organic additives [13, 15]. The migration of  $\text{Cu}^{2+}$  ions is a key factor to improve the quality of Cu deposits. Several circulation modes of the electrolyte have been attempted to accelerate the diffusion of  $\text{Cu}^{2+}$  ions, including the use of a jet flow, a rotating cylinder electrode, and the Lorentz force as well as redesigning the electrolytic cells [13, 15-19]. To date, the preparation of compact, smooth and dendrite-free Cu deposits is still a challenge in the recovery of Cu metal.

The objective of this work is to prepare compact and smooth Cu deposits by electrowinning  $\text{Cu}^{2+}$  ions in a  $\text{CuSO}_4\text{-H}_2\text{SO}_4$  solution. The mass transfer of Cu ions and the growth of Cu grains were promoted dynamically by employing flowing bubbles and magnetic agitation during the electrowinning process. The microstructure and crystal orientation of the deposit were also modified. Organic additives were avoided to eliminate the contamination of Cu deposits. Furthermore, the reaction mechanism for the reduction of  $\text{Cu}^{2+}$  ions and the growth of Cu deposits was investigated.

## 2. EXPERIMENTAL

$\text{CuSO}_4\cdot5\text{H}_2\text{O}$  (Sinopharm Chemical Reagent Co., Ltd) and  $\text{H}_2\text{SO}_4$  ( $2.04 \text{ mol}\cdot\text{L}^{-1}$ ) were dissolved in deionized water to prepare an acidic solution for electrowinning  $\text{Cu}^{2+}$  ions. The concentrations of  $\text{Cu}^{2+}$  ions and  $\text{H}_2\text{SO}_4$  were  $0.39 \text{ mol}\cdot\text{L}^{-1}$  and  $1.74 \text{ mol}\cdot\text{L}^{-1}$ , respectively. All chemicals used in this work were of analytical grade. A rectangular Ti sheet ( $1.5 \text{ cm} \times 2 \text{ cm} \times 0.1 \text{ cm}$ ) was polished mechanically and subsequently washed ultrasonically to obtain a mirror-like surface. The Ti sheet was connected to an electric wire as the cathode. A Cu plate ( $5 \text{ cm} \times 4 \text{ cm} \times 0.5 \text{ cm}$ ) was employed as the anode, which was also treated similarly to prepare a smooth surface. A cylindrical cell (diameter: 9 cm, height: 9 cm) was filled with 0.5 L of the acidic solution.

Electrowinning of  $\text{Cu}^{2+}$  ions was carried out with a current density ranging from 5 to  $40 \text{ mA}\cdot\text{cm}^{-2}$ . The temperature of the electrolyte was maintained at  $32^\circ\text{C}$ . A rotor (diameter: 0.8 cm, length: 2 cm) was placed under the Ti cathode, which was approximately 4 cm under the cathode. The speed was adjusted magnetically in the electrowinning process. Alternatively, the rotor was replaced by a porous

ceramic sieve (size: 5 cm, average diameter of the holes:  $\sim 70 \mu\text{m}$ ) to generate an upward flow of gas bubbles in the electrolytic cell. High-purity Ar and CO<sub>2</sub> were used as the source of gas bubbles.

Electrochemical behavior of Cu<sup>2+</sup> ions was investigated in a three-electrode cell using a CHI1140C potentiostat. The concentration of CuSO<sub>4</sub> in the solution was 0.01 mol·L<sup>-1</sup> (pH=1). Na<sub>2</sub>SO<sub>4</sub> (concentration: 0.01 mol·L<sup>-1</sup>) was added into the solution as a supporting electrolyte. A glassy carbon rod embedded in a Teflon holder (exposed area: 0.071cm<sup>2</sup>) was utilized as the working electrode. A platinum plate (3 cm  $\times$  3 cm  $\times$  0.1 cm) and a saturated calomel electrode (SCE) were used as the counter electrode and the reference electrode, respectively. Cyclic voltammograms were measured to investigate reducing process of Cu<sup>2+</sup> ions. Chronoamperometry was performed to study the nucleation and growth of Cu deposits.

The phase composition of the samples prepared under various conditions was determined by a Rigaku D/Max-2500PC X-ray diffractometer (XRD,  $\lambda = 1.54059 \text{ \AA}$ ). Morphological observation was conducted with a scanning electron microscope (SEM, FEI Quanta FEG 250).

### 3. RESULTS AND DISCUSSION

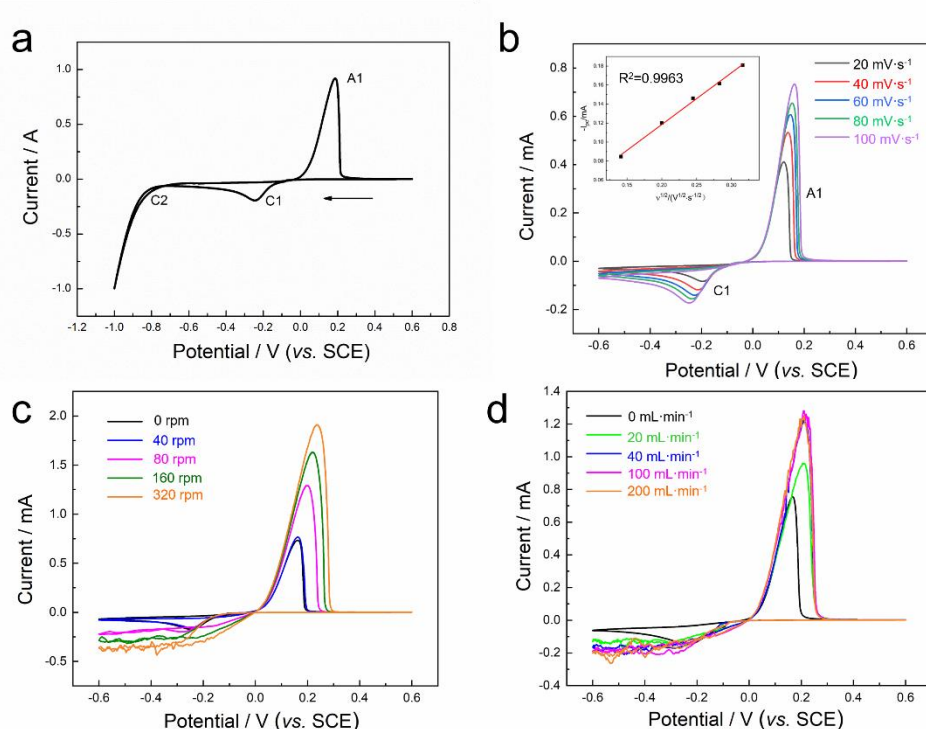


**Figure 1.** Cyclic voltammograms recorded (a) in a 0.01 M CuSO<sub>4</sub> + 0.1 M Na<sub>2</sub>SO<sub>4</sub> solution (pH = 1, scan rate: 100 mV·s<sup>-1</sup>); (b) at various scan rates in a static solution (0.01 M CuSO<sub>4</sub> + 0.1 M Na<sub>2</sub>SO<sub>4</sub>, pH = 1); (c) in a solution magnetically agitated at various speeds (0.01 M CuSO<sub>4</sub> + 0.1 M Na<sub>2</sub>SO<sub>4</sub>, pH = 1, scan rate: 100 mV·s<sup>-1</sup>); (d) in a solution stirred with flowing bubbles as various rates (0.01 M CuSO<sub>4</sub> + 0.1 M Na<sub>2</sub>SO<sub>4</sub>, pH = 1, scan rate: 100 mV·s<sup>-1</sup>).

Figure 1a shows a representative cyclic voltammogram (CV) of Cu<sup>2+</sup> ions in an acidic sulfate solution (0.01 M CuSO<sub>4</sub> + 0.1 M Na<sub>2</sub>SO<sub>4</sub>, pH = 1). The CV curve started negatively at 0.60 V (vs. SCE) and was reversed at -1.0 V for the anodic scan. During the negative scan, a current peak (C1) centered at about -0.25 V (vs. SCE) can be observed, which corresponds to the reduction from Cu<sup>2+</sup> to Cu (Eq. 1) [20-24]. Correspondingly, an anodic peak (A1) at approximately -0.1 V is related to the dissolution of deposited Cu to Cu<sup>2+</sup> ions on the working electrode [23, 25]. The gap in potentials for the deposition and dissolution of Cu is in good agreement with the value in the literature [26]. The CV curve characterized as a crossover of the cathodic and anodic branches at about -0.1 V, which is a fingerprint of the formation of copper nuclei on the electrode [25-27]. This phenomenon is attributed to the dynamic characteristics of the deposition and oxidation of copper species. An overpotential is needed for the deposition of Cu due to the structural mismatch of glassy carbon and Cu, which is not a requisite for the reoxidation of Cu deposits [25, 27, 28]. Cathodic current (C2) starting at about -0.8 V is ascribed to the reduction of H<sup>+</sup> ions (Eq. 2) [22]. This means that the release of H<sub>2</sub> is less favorable since C2 is far more negative than the reduction of Cu<sup>2+</sup> ions (C1).

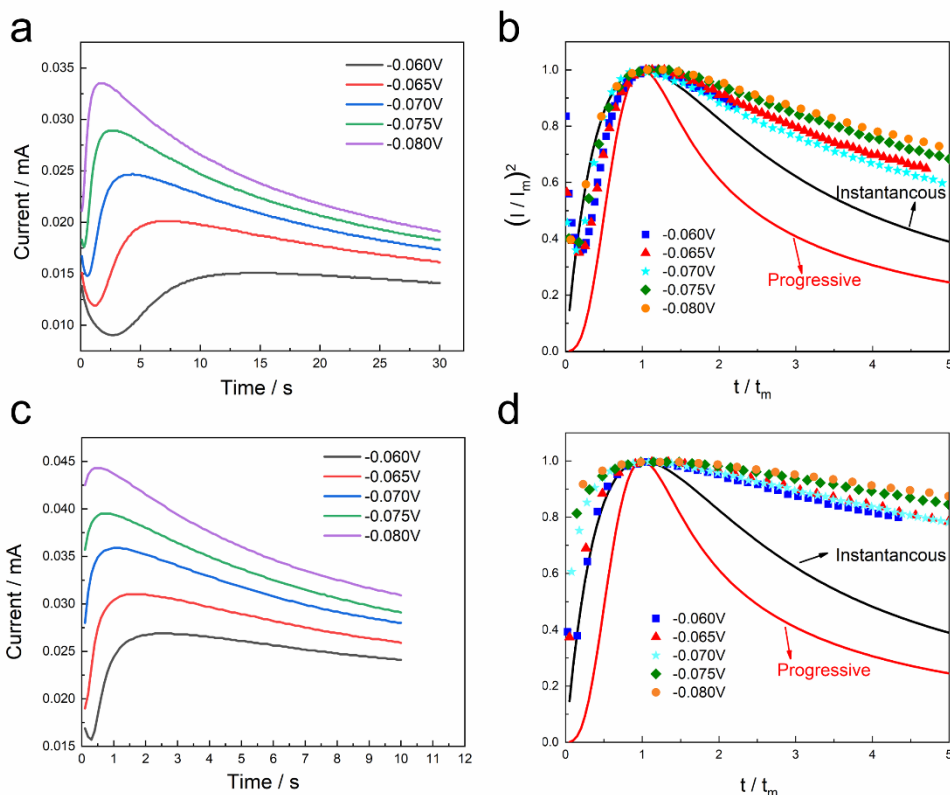


Figure 1b shows CV curves measured at various scan rates from 20 to 100 mV·s<sup>-1</sup>. The intensity of A1 ( $I_{pc}$ ) was plotted as a function of the square root of scan rates ( $\nu^{1/2}$ ) (the inset in Figure 1b). The linear relationship between  $I_{pc}$  and  $\nu^{1/2}$  indicates that the reduction from Cu<sup>2+</sup> to Cu is controlled by mass transfer [25, 28]. Moreover, the value of current at  $\nu^{1/2} = 0$  reveals the involvement of a nucleation process during the reduction. It is controlled by mass transport of electroactive species [25, 28].

The diffusion of Cu<sup>2+</sup> ions deserves more attention during the electrowinning process. As reported by our previous work [29], a flow of gaseous bubbles is an effective method to accelerate the migration of Co<sup>2+</sup> ions, so a flow of bubbles was introduced into the electrowinning of Cu<sup>2+</sup> ions. In addition, magnetic agitation was also employed to promote mass transportation of Cu<sup>2+</sup> ions. Figure 1c shows CV curves recorded with the assistance of magnetic agitation. The cathodic current obtained at 40 rpm did not increase obviously from the current recorded in the static electrolyte since the rotating speed was not adequate to influence the diffusion of Cu<sup>2+</sup> ions. Subsequently, a limiting cathodic current appeared from -0.25 V downwards when the rotating speed was higher than 80 rpm. This implies that Cu<sup>2+</sup> ions consumed in the reduction can be simultaneously supplied by agitating the ions towards the substrate. The limiting current increased with the rotating speed of the rotor. Meanwhile, the oxidation peak of Cu deposit was also enhanced. The phenomenon is similar to the phenomenon of reducing tin ions on a rotating electrode [30]. Both magnetic agitation and a rotating electrode can accelerate the transport of electroactive species during the reduction processes. However, magnetic agitation may be more effective in driving Cu<sup>2+</sup> ions towards the substrate by stirring the electrolyte. Similarly, a limiting cathodic current can be observed once a flow of Ar bubbles is introduced into the reduction process (Figure 1d). This means that the gaseous bubbles can also promote the transport of Cu<sup>2+</sup> ions for electrowinning.

Current transients were recorded by applying the potentials in the range of the descending branch

of C1 (Figure 2a). The current increased abruptly after the charging of the double layer within a short duration and decayed gradually after a maximum value. The evolution of current transients can be characterized by the typical mode proposed by Scharifker and Hill [3, 30, 31], in which a new phase was formed electrochemically by a diffusion-controlled process of depositing species from the bulk electrolyte. As a three-dimensional nucleation process controlled by hemispherical diffusion, it can be classified as instantaneous and progressive nucleation [3, 29, 31]. The models can be described by the nondimensional expressions in Eqs. (4) and (5), where  $I$  is the current and  $I_m$  is the maximum value of the current.  $t$  represents time, and  $t_m$  is the time corresponding to  $I_m$ .



**Figure 2.** (a) Current transients and (b) nondimensional  $(I/I_m)^2$  vs.  $t/t_m$  curves obtained for the reduction of  $\text{Cu}^{2+}$  ions in a static solution ( $0.01 \text{ M CuSO}_4 + 0.1 \text{ M Na}_2\text{SO}_4$ , pH = 1); (c) current transients and (d) nondimensional  $(I/I_m)^2$  vs.  $t/t_m$  curves for the reduction of  $\text{Cu}^{2+}$  ions in a magnetically agitated solution (40 rpm,  $0.01 \text{ M CuSO}_4 + 0.1 \text{ M Na}_2\text{SO}_4$ , pH = 1).

For instantaneous nucleation

$$\left(\frac{I}{I_m}\right)^2 = 1.9542 \left(\frac{t}{t_m}\right)^{-1} \left\{ 1 - \exp \left[ -1.2564 \left(\frac{t}{t_m}\right) \right] \right\}^{-2} \quad (4)$$

and for progressive nucleation

$$\left(\frac{I}{I_m}\right)^2 = 1.2254 \left(\frac{t}{t_m}\right)^{-1} \left\{ 1 - \exp \left[ -2.3367 \left( \frac{t}{t_m} \right)^2 \right] \right\}^{-2} \quad (5)$$

The theoretical curves and the corresponding data were plotted together to determine the mode of nucleation that occurred in the electrochemical process (Figure 2b). Initially, the experimental data fit reasonably well to the instantaneous nucleation model. The nucleation model for Cu<sup>2+</sup> reduction is predominantly instantaneous. However, the data deviate from the instantaneous nucleation model with the extension of  $t/t_m$ , where the values of  $(I/I_m)^2$  are higher than the theoretical values predicted by the model. The deviation is related to several factors, such as the pH values, the concentration of Cu<sup>2+</sup> and the geometry of copper nuclei [20, 27]. The current measured in a magnetically agitated solution is relatively higher than those in Figure 2a. Moreover, the decay of current following the maximal value is less apparent even though the measurements were conducted at the same potential. It indicates that the mass transfer of Cu<sup>2+</sup> ions was promoted by magnetic agitation. Though the nucleation mode was not changed by the agitation (Figure 2d), the characteristics of Cu nuclei may change because the geometry of copper nuclei is related to the variation in  $(I/I_m)$  from the theoretical mode [20, 27].

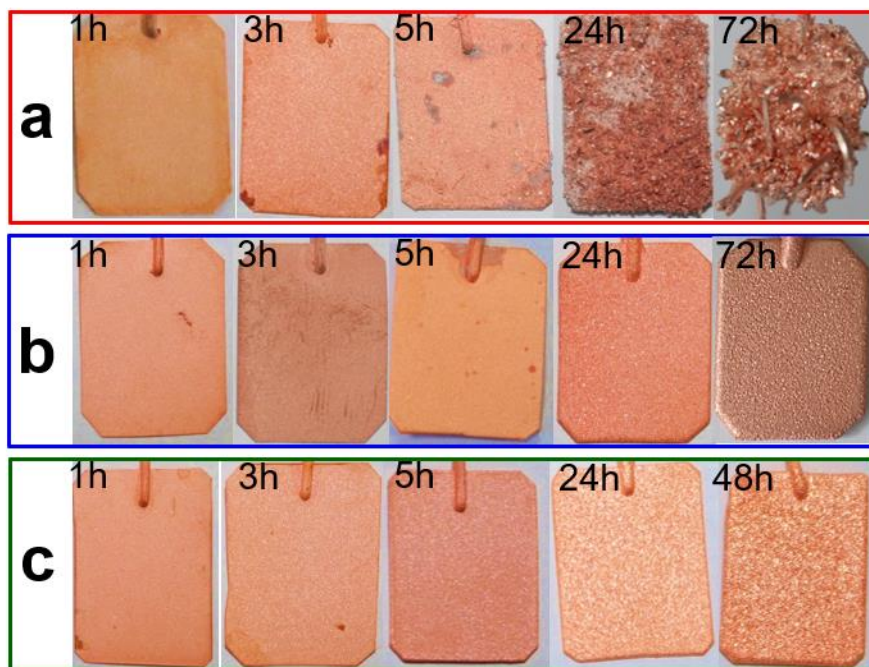


**Figure 3.** Digital photos of the samples prepared for various durations in (a) static; (b) magnetically agitated (480 rpm); (c) bubbly stirred (150 mL·min<sup>-1</sup>) electrolyte. (Current density: at 10 mA·cm<sup>-2</sup>, composition of electrolyte: 0.39 mol·L<sup>-1</sup> Cu<sub>2</sub>SO<sub>4</sub> and 1.74 mol·L<sup>-1</sup> H<sub>2</sub>SO<sub>4</sub>, T = 32 °C)

Electrowinning of Cu<sup>2+</sup> ions was carried out in a 0.39 M CuSO<sub>4</sub> + 1.74 M H<sub>2</sub>SO<sub>4</sub> solution with a current density of 10 mA·cm<sup>-2</sup>. Figure 3a exhibits digital photos of the samples obtained for various durations in a static solution. The Cu deposit presents a smooth and compact surface at the initial stage of electrowinning (1 h and 3 h), which is consistent with the deposit obtained in the literature [1, 3]. The smooth surface may be attributed to the fine primary crystals formed on the substrate. Then some

dendrites appeared at the edge of the sample (5 h). This phenomenon is due to the inhomogeneous distribution of current on the substrate. After 24 h of electrowinning, most of the surface was covered by dendritic particles, generating a loose and porous microstructure. Then many crystals grew extendedly towards the electrolyte to form a spinous morphology when the duration was 72 h. In general, dendritic growth is a common phenomenon once electrowinning is carried out in a static solution. This phenomenon may quite differ from the results in previous work since organic additives were not utilized in this study [32]. The formation of dendrites involves the inclusion of impurities in Cu deposits, which severely influences the purity and quality of the product. Moreover, it was found that the  $\text{CuSO}_4$  electrolyte tended to be entrapped in the porous deposit even if it was thoroughly rinsed with deionized water.

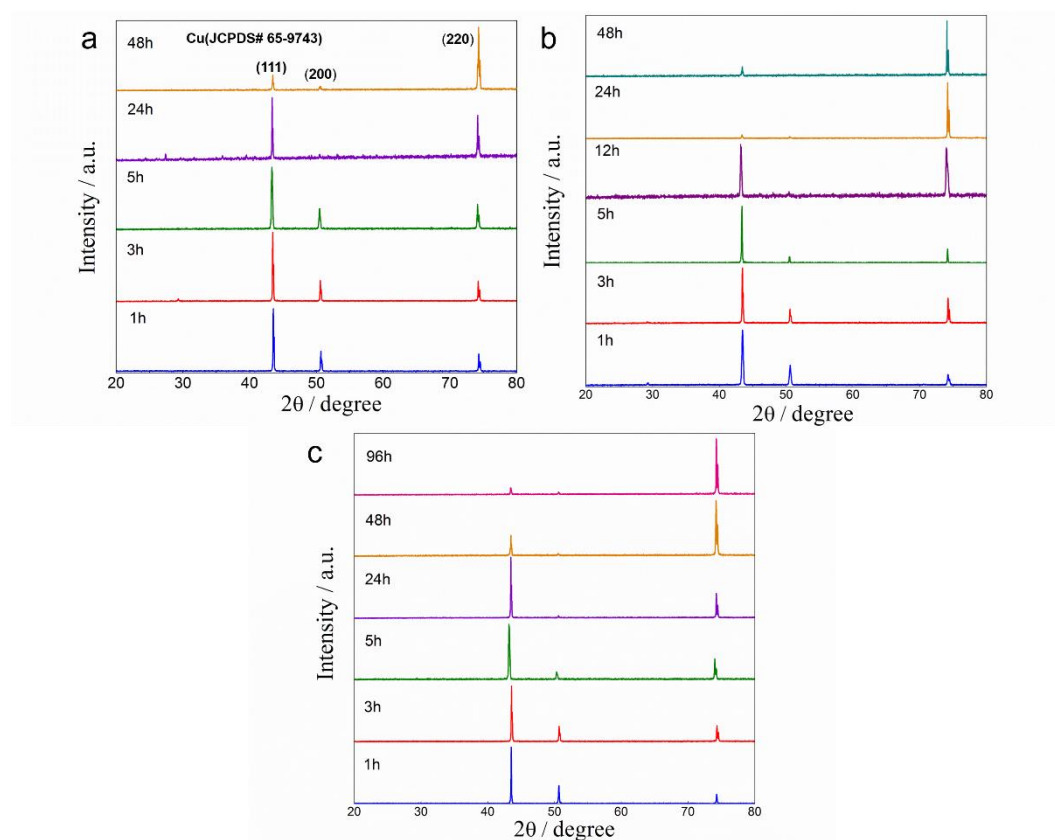


**Figure 4.** XRD patterns of the samples prepared for various durations in (a) static; (b) magnetically agitated (480 rpm); (c) bubbly stirred ( $150 \text{ mL}\cdot\text{min}^{-1}$ ) electrolyte. (Current density: at  $10 \text{ mA}\cdot\text{cm}^{-2}$ , composition of electrolyte:  $0.39 \text{ mol}\cdot\text{L}^{-1} \text{ Cu}_2\text{SO}_4$  and  $1.74 \text{ mol}\cdot\text{L}^{-1} \text{ H}_2\text{SO}_4$ ,  $T = 32^\circ\text{C}$ )

Subsequently, magnetic agitation (480 rpm) and flowing bubbles ( $150 \text{ ml}\cdot\text{min}^{-1}$ ) were employed for electrowinning of  $\text{Cu}^{2+}$  ions. The dendritic growth of the copper deposits basically disappeared once the solution was agitated magnetically by a rotor (Figure 3b). A compact Cu deposit was prepared, although some geological concavities and convexities existed on the surface. As well, Cu deposit without concavities and convexities can be produced once an upwards flow of bubbles is utilized in the

electrowinning process (Figure 3c). It can be concluded that both magnetic agitation and flowing bubbles can eliminate the growth of dendrites to produce compact deposits, in which a bubbly flow is more effective. This issue can be explained by the improvement of micron-sized bubbles for the diffusion of Cu<sup>2+</sup> ions and the growth of Cu crystals in comparison to a rotating rotor.

Figure 4a shows XRD patterns of the samples electrowon for various durations in a static solution. Three typical diffraction peaks were detected at approximately 43.3°, 50.4° and 74.1°, which can be assigned to the (111), (200) and (220) planes of Cu with a cubic structure (JCPDS#04-836), respectively. Initially, the (111) plane was the most preferred orientation (1 and 3 h). Then, the (220) plane started to grow preferentially with the extension of duration (24 h). After 48 h of electrowinning, the (220) diffraction peak became the most predominant, and the (111) diffraction peak changed to a low bump. This transition implies that the preferential growth of copper deposits changed at the electrowinning proceeded. The (200) plane is the most preferred once organic or inorganic impurities do not exist in the electrolyte [3, 33].

The transformation of preferential growth between the (111) and (220) planes also occurred when electrowinning was conducted in the magnetically agitated solution (480 rpm). The (111) plane grew preferentially during the initial electrowinning since the nucleation mode of Cu was not changed by employing magnetic agitation (Figure 4b). Nevertheless, the preferential growth of the (220) plane was obvious after 12 h of electrowinning. The diffraction peaks of the (220) plane are sharper and better defined than those in Figure 4a. These aspects prove that magnetic agitation of the electrolyte can promote the growth of copper crystals on the Ti substrate. This consequence can also be achieved by introducing upward flowing bubbles (150 ml·min<sup>-1</sup>) into the electrowinning process (Figure 4c). The full width half maximum (FWHM) of the (220) plane for the samples deposited for 48 h was measured to estimate the crystallinity of Cu deposits. The FWHM of the (220) plane for the deposit prepared by magnetic agitation (0.071°) or flowing bubbles (0.103°) is less than the value for the deposit obtained in a static electrolyte (0.116°). Correspondingly, the crystal sizes of the Cu deposit are 423.9, 292.2 and 259.4 nm, according to the Debye-Scherrer formula. The agitation and flowing bubbles are available for the evolution of crystals of Cu deposits. In comparison, magnetic agitation is more effective in promoting the evolution of copper crystals. In addition, the size of Cu crystals is obviously larger than those reported in the literature [3, 34, 35].

Figures 5a-5d show SEM images of the samples electrowon for 1, 3, 24 and 48 h in a static solution. The deposit after 1 h of electrowinning is composed of bulk particles less than 10 µm (Figure 5a). The Cu particles are not uniform, which is in agreement with the results in the literature [15, 33, 36]. In addition, many particles less than 1 µm are present along the boundaries of the bulk particles (the inset in Figure 5a), forming an inhomogeneous morphology. This phenomenon proves that Cu nuclei were continuously formed in this period. Subsequently, both the bulk particles and the smaller particles evolved into larger particles when the duration was extended to 3 h (Figure 5b). A coarse and porous structure was formed once dendritic particles appeared on the substrate (Figures 5c and 5d). The dendritic deposit was easily detached from the substrate and aggregated at the bottom of the electrolytic cell. The coarse and porous structure will decrease the purity of the Cu deposits since the impurities and electrolyte can be trapped inside.

The morphologies of the samples electrowon for 1, 3, 24 and 48 h in a magnetically agitated

solution are shown in Figures 5e-5h. The size of particles prepared for 1 h (Figure 5e) did not vary obviously in comparison with that prepared in a static solution (Figure 5a). However, Cu nuclei near the boundaries of bulk particles are less detectable (the insets in Figures 5e-5f). The particles deposited for longer durations (Figures 5f-5h) are more uniform than those in Figures 5b-5d. This morphological evolution of the Cu deposit is similar to that of the Cu deposit by introducing a jet flow into the electrowinning of  $\text{Cu}^{2+}$  ions [15]. Furthermore, dendritic growth of the Cu deposits did not appear on the substrate. The secondary nucleation of Cu along the boundaries of the deposits was effectively restrained with the assistance of agitation. The porous structure induced by dendritic growth was also avoided. As indicated by the inset in Figures 5f-5g, many small convexities can be observed on the surface of Cu particles. The reason for the formation of convexities is probably related to the direction of the agitation. This situation can be improved once the duration is extended to 48 h (Figure 5h).

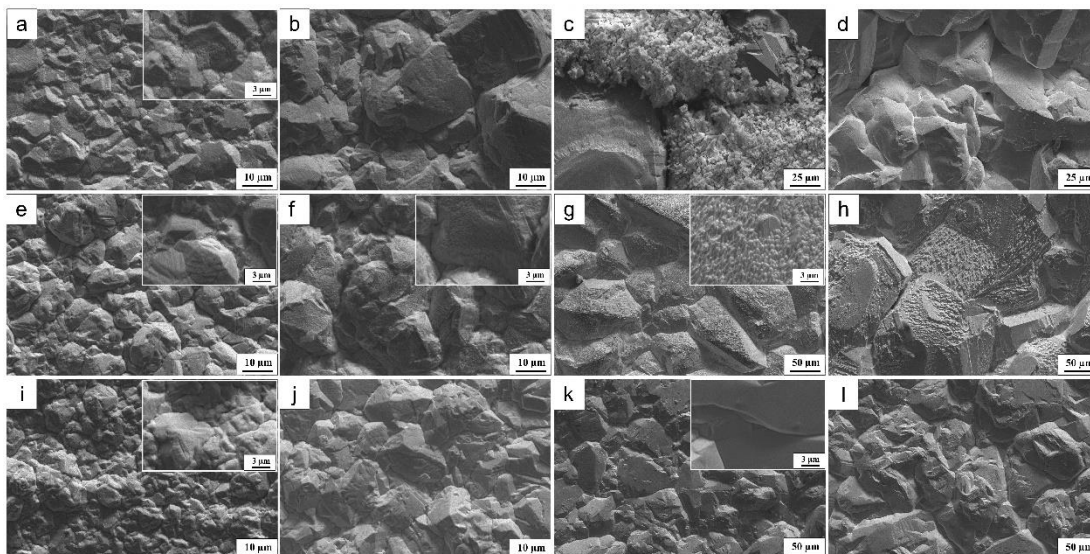


**Figure 5.** SEM and enlarged SEM images of the samples prepared at  $10 \text{ mA}\cdot\text{cm}^{-2}$  for (a) 1; (b) 3; (c) 24; (d) 48 h in a static electrolyte; (e) 1; (f) 3; (g) 24; (h) 48 h in a magnetically agitated electrolyte (480 rpm); (i) 1; (j) 3; (k) 24; (l) 48 h in a bubbly stirred ( $150 \text{ mL}\cdot\text{min}^{-1}$ ) electrolyte. (Current density: at  $10 \text{ mA}\cdot\text{cm}^{-2}$ , composition of electrolyte:  $0.39 \text{ mol}\cdot\text{L}^{-1} \text{ Cu}_2\text{SO}_4$  and  $1.74 \text{ mol}\cdot\text{L}^{-1} \text{ H}_2\text{SO}_4$ ,  $T = 32^\circ\text{C}$ )

Figures 5i-5l present SEM images of the samples deposited for 1, 3, 24 and 48 h after the introduction of flowing bubbles. The particles prepared for 1 h (Figure 5i) are relatively smaller and more uniform than those in Figures 5a and 5e. This means that the flowing bubbles are more beneficial for the nucleation of Cu at the initial stage of electrowinning. Then, the particles evolved into bigger crystals as the electrowinning proceeded (Figure 5j and 5k). The deposit produced for 48 h is compact and composed of Cu crystals larger than  $50 \mu\text{m}$  (Figure 5l). Furthermore, secondary nucleation along the boundaries of Cu crystals was basically prevented (the insets in Figures 5i and 5j). The deposit consists of well-defined crystals with the assistance of flowing bubbles.

The weight of the Cu deposits was measured, and the current efficiency was calculated by comparing the weight with the charges consumed during the electrowinning processes (Figure 6a). The

weight of Cu deposits gained in different processes is almost the same. Additionally, the current efficiency is generally maintained at more than 99 %. Figure 6b displays the variation in cell voltage after 24 h of electrowinning without and with the assistance of magnetic agitation/flowing bubbles. The cell voltages increased to some extent after the introduction of magnetic agitation or upward flowing bubbles. This may be attributed to the existence of whirlpools or micron-sized bubbles in the cell, which enhance the resistance between the anode and the cathode.

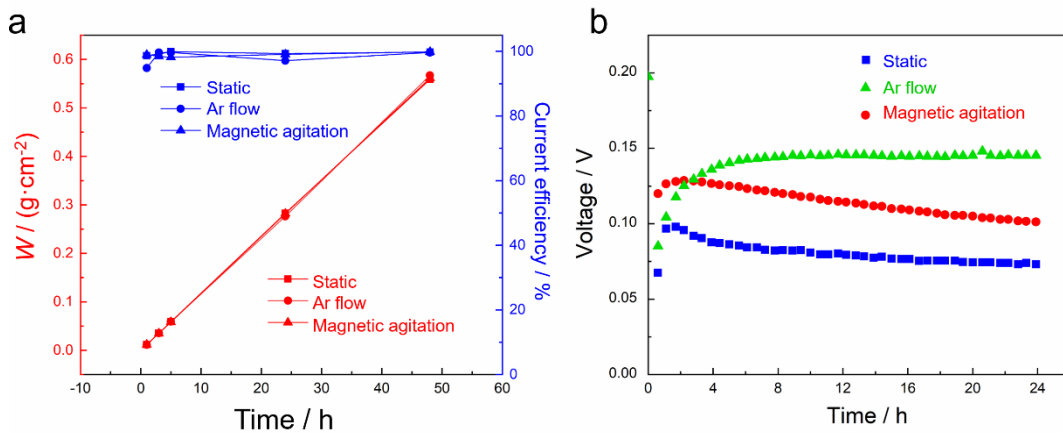


**Figure 6.** (a) Weight of Cu deposit and current efficiency in various electrowinning processes; (b) variation in cell voltage recorded during 24 h of electrowinning.

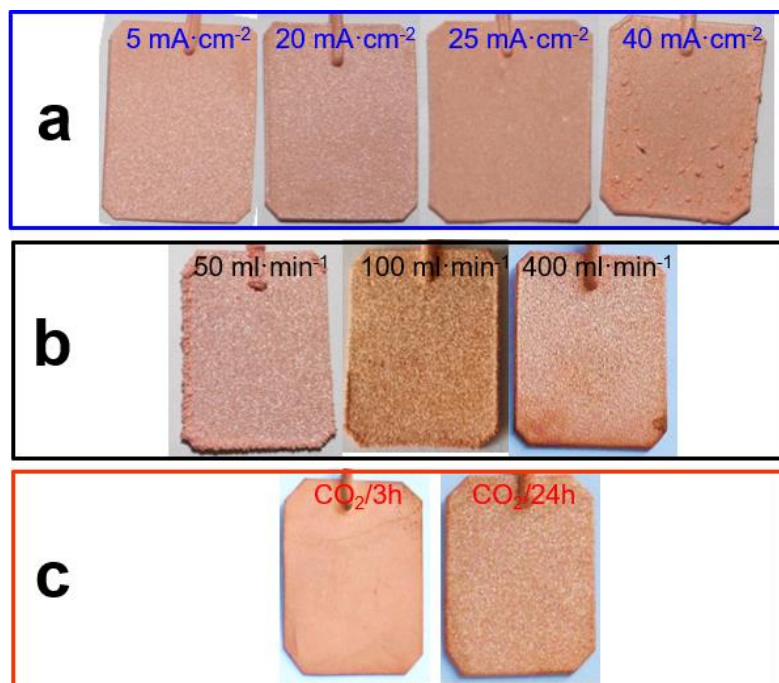


**Figure 7.** Digital photos of the samples obtained (a) at various current densities for 5 h (flow rate: 150  $\text{ml} \cdot \text{min}^{-2}$ ,  $T = 32^\circ\text{C}$ ); (b) at various flow rates of gas for 24 h (current density: 10  $\text{mA} \cdot \text{cm}^{-2}$ ,  $T = 32^\circ\text{C}$ ); (d) with the assistance of  $\text{CO}_2$  bubbles for 3 and 24 h (flow rate: 150  $\text{ml} \cdot \text{min}^{-2}$ , current density: 10  $\text{mA} \cdot \text{cm}^{-2}$ ,  $T = 32^\circ\text{C}$ ).

The upward-flowing bubbles are available for the development of compact deposits composed of uniform and well-defined crystals. To provide more evidence for this deduction, Cu samples were also prepared by varying the electrowinning parameters. Figure 7a shows digital photos of the samples prepared at current densities of 5, 20, 25 and 40 mA·cm<sup>-2</sup> with the assistance of flowing bubbles (150 ml·min<sup>-1</sup>). Uniform and compact samples were produced below 25 mA·cm<sup>-2</sup>. However, some nodular particles started to appear on the substrate when the current density was 40 mA·cm<sup>-2</sup>. It seems that the effect of flowing bubbles was limited since the growth of secondary nuclei and the uniform current distribution probably took place at higher current densities. Afterwards, the flow rate of bubbles was adjusted to 50, 100 and 400 ml·min<sup>-1</sup> for 24 h (Figure 7b). The dendritic growth of Cu was relieved once the bubbly flow was introduced into electrowinning at a rate of 50 ml·min<sup>-1</sup>. This trend is more obvious by increasing the flow rate. Finally, the source of gaseous bubbles was replaced by CO<sub>2</sub>. Compact and smooth Cu deposits were also prepared with the assistance of CO<sub>2</sub> bubbles (Figure 9c). Therefore, the positive effect of flowing bubbles may be derived from the interaction between the micron-sized bubbles and Cu nuclei instead of the type of molecules inside the bubbles.

#### 4. CONCLUSIONS

Electrowinning of Cu<sup>2+</sup> ions was conducted in a CuSO<sub>4</sub>-H<sub>2</sub>SO<sub>4</sub> solution by employing magnetic agitation and upward flowing bubbles in the process. Mass transport of Cu<sup>2+</sup> ions towards the cathode was effectively accelerated by agitation and micron-sized bubbles. Primary nucleation and the subsequent growth of Cu deposits can be promoted, though the instantaneous mode of nucleation was not altered. Moreover, the occurrence of secondary nucleation on the deposited Cu particles was hindered. The growth of dendritic particles that commonly occurs in static solution can also be eliminated. Both the morphology and the preferential growth of Cu deposits can be modified by magnetic agitation and flowing bubbles. Finally, a compact and smooth Cu deposit consisting of well-defined crystals can be achieved, which is beneficial for producing high-purity Cu. The positive effect of flowing bubbles is attributed to the dynamic interaction between the micron-sized bubbles and the Cu nuclei.

#### ACKNOWLEDGEMENTS

This work was financially supported by the National Key Research and Development Program of China (Grant No. 2017YFB0305401) for financial support.

#### References

1. A. Baral, C.K. Sarangi, B.C. Tripathy, I.N. Bhattacharya and T. Subbaiah, *Hydrometallurgy*, 146 (2014) 8.
2. S. Jafari, M. Kiviluoma, T. Kalliomäki, E. Klindtworth, A.T. Aji, J. Aromaa, B.P. Wilson and M. Lundström, *Int. J. Miner. Process.*, 168 (2017) 109.
3. L.K. Wu, C.C. Li, Z.F. Zhang, H.Z. Cao, J. Xue and G.Q. Zheng, *J. Electrochem. Soc.*, 164 (2017) D451.
4. F. Qiao and A.C. West, *Electrochim. Acta*, 150 (2014) 8.

5. R. Seakr, *T. Nonferr. Metal. Soc.*, 27 (2017) 1423.
6. T. Kalliomaki, B.P. Wilson, J. Aromaa and M. Lundstrom, *Miner. Eng.*, 134 (2019) 381.
7. A. Artzer, M. Moats and J. Bender, *JOM*, 70 (2018) 2033.
8. W. Zeng, J. Werner and M.L. Free, *Hydrometallurgy*, 156 (2015) 232.
9. A. Owais, M.A.H. Gepreel and E. Ahmed, *Hydrometallurgy*, 152 (2015) 55.
10. B. Veilleux, A.M. Lafront and E. Ghali, *J. Appl. Electrochem.*, 31 (2001) 1017.
11. A. Suzuki, S. Oue, S. Kobayashi and H. Nakano, *Mater. Trans.*, 58 (2017) 1538.
12. B. Veilleux, A.M. Lafront and E. Ghali, *Can. Metall. Q.*, 41 (2002) 47.
13. C. Fabian, M.J. Ridd and M. Sheehan, *Hydrometallurgy*, 84 (2006) 256.
14. T. Haba, K. Ikeda and K. Uosaki, *Electrochim. Commun.*, 98 (2019) 19.
15. H. Wang, Q. Wang, W. Xia and B. Ren, *Metals*, 8 (2018) 833.
16. W.Z. Zeng, M.L. Free and S.J. Wang, *ECS Trans.*, 72 (2016) 23.
17. W.Z. Zeng, S.J. Wang and M.L. Free, *JOM*, 69 (2017) 1876.
18. S. Kawai and T. Miyazawa, *Miner. Eng.*, 63 (2014) 81.
19. M. Najminoori, A. Mohebbi, K. Afroz and B.G. Arabi, *Chem. Eng. Sci.*, 199 (2019) 1.
20. A.E. Bolzán, *Electrochim. Acta*, 113 (2013) 706.
21. N.N. Che Isa and Y. Mohd, *Solid State Sci. Technol.*, 25 (2017) 103.
22. S.K. Ghosh, *Electrochim. Acta*, 53 (2008) 8070.
23. T. Ishizaki, D. Yata and A. Fuwa, *Mater. Trans.*, 44, (2003) 1583.
24. M.R. Majidi, K. Asadpour-Zeynali and B. Hafezi, *Electrochim. Acta*, 54 (2009) 1119.
25. D. Grujicic and B. Pesic, *Electrochim. Acta*, 50 (2005) 4426.
26. E. Kazimierska, E. Andreoli and A.R. Barron, *J. Appl. Electrochem.*, 49 (2019) 731.
27. D. Grujicic and B. Pesic, *Electrochim. Acta*, 47 (2002) 2901.
28. L. Huang, E. S. Lee and K.B. Kim, *Colloids Surf. A*, 262 (2005) 125.
29. Q. Song, Y. Zhao, C. Wang, H. Xie, H. Yin and Z. Ning, *Hydrometallurgy*, 189 (2019) 105111.
30. L.A. Azpeitia, C.A. Gervasi and A.E. Bolzán, *Electrochim. Acta*, 298 (2019) 400.
31. B. Scharifker and G. Hills, *Electrochim. Acta*, 28 (1983) 879.
32. C. Fabian, M.J. Ridd and M. Sheehan, *Hydrometallurgy*, 86 (2007) 44.
33. B. Panda, S.C. Das and R.K. Panda, *Metall. Mater. Trans. B*, 34B (2003) 813.
34. N.D. Nikolic, L. Avramovic, E.R. Ivanovic, V.M. Maksimovic, Z. Bascarevic and N. Ignjatovic, *Trans. Nonferrous Met. Soc. China*, 29 (2019) 1275.
35. R. Sekar, *Trans. Nonferrous Met. Soc. China*, 27 (2017) 1665.
36. B. Panda and S.C. Das, *Hydrometallurgy*, 59 (2001) 55.